

A High-Precision Angle Encoder for a 10-m Submillimeter Antenna

Nobuharu UKITA*, Hajime EZAWA*, Hisashi MIMURA†, Akira SUGANUMA‡,
Kanji KITAZAWA†, Tadashi MASUDA‡, Noboru KAWAGUCHI§, Ryuichi SUGIYAMA§,
and Keizou MIYAWAKI§

(Received Oct. 16, 2000)

Abstract

We report measurements of angle error characteristics of new high-precision multi-speed resolvers developed for a 10-m submillimeter telescope of Nobeyama Radio Observatory. We have found the resolvers have an accuracy of 0.03" rms and 0.26" peak-to-peak, which is well below the error budget assigned to the angle encoder in the LMSA/ALMA project (0.15 – 0.2"). The error pattern in the raw readout had simple characteristics and was only composed of a few Fourier components which are associated with the number of winding poles and core slot number of stator. The 4" peak-to-peak error in the raw readout is reduced to less than 1/15 by the PROM correction. We have also found that shaft misalignment causes only small changes of error pattern (0.08" error per 0.10 mm shaft misalignment), which enables us to install the resolver simply by the fitting. The temperature dependence of error pattern also seems to be small enough for the operation temperature range specified in the project.

Key words: Radio telescope, angle encoder, resolver.

1. Introduction

The angle detection device is a key instrument for the accuracy of pointing/tracking of a radio telescope, because radio telescopes are usually obliged to make blind pointing using only angle encoder readouts. The specifications imposed on recent high-precision antennas are demanding and challenging. For example, the antennas of a 10-12 m diameter for the Large Millimeter/Submillimeter Array (LMSA) project (e.g., Ishiguro et al. 1998) and the Atacama Large Millimeter Array (ALMA) project (e.g., Cheng and Kingsley 1998) are specified to have a pointing/tracking accuracy of better than 0.7 – 0.8". The error budget assigned to the angle encoder is as small as 0.15 – 0.2".

Nobeyama Radio Observatory (NRO)[¶] has constructed a 10-m submillimeter antenna which has been designed as an experimental antenna for the LMSA project (Ukita et al. 2000). The angle encoders we employed are multi-speed resolvers (resolver for short)

with a 25-bit resolution (LSB = 0.039"). They are not only high accuracy, but are also capable for reading out absolute angles. Furthermore, they should have high reliability, because the telescope is operated in harsh conditions, namely in the open air, at an elevation of 4800 m, and in the desert at a remote site. The resolver would be very competent for this job among various types of angle encoders (e.g., an optical rotary encoder), since it has a simple robust structure and simple error characteristics.

In 1988, we developed a resolver system with an accuracy of 0.4" rms (Ukita and Tsuboi 1994). As a result of continuous improvements of high accuracy resolvers in a subsequent decade, the performance can now be discussed on the order of 10 milli-arcsecond (mas). Such efforts include new winding arrangements and angle error studies based on magnetic field analyses of a resolver with a finite element method (e.g., Masaki, 1999) and development of high accuracy angle calibration system (Masuda and Kajitani 1993).

* Nobeyama Radio Observatory, Minamimaki, Minamisaku, Nagano, Japan

† Tamagawa Seiki Co, 1879, Ohyasumi, Iida, Nagano, Japan

‡ Shizuoka Institute of Science and Technology, 2200-2, Toyosawa, Fukuroi, Shizuoka, Japan

§ Mitsubishi Electric Co, 8-1-1, Tsukamoto, Amagasaki, Hyogo, Japan

¶ Nobeyama Radio Observatory is a branch of the National Astronomical Observatory, Japan, an inter-university research operated by the Ministry of Education, Science, Sports, and Culture, Japan.

This report describes our high-precision resolver system and its performance. Section 2 explains our resolver system and the basic principle on which the device works. In section 3, we show that our encoder system has achieved an accuracy of 30 mas rms. We have also made various measurements of error characteristics of the system, which will be useful in maintaining the system accuracy and in shooting troubles of the system. The achieved high accuracy of 30 mas rms would greatly help us to measure dynamical behaviors of the antenna system, those due to dynamic loadings from wind turbulence, seismic ground motion, and periodic mechanical loadings from telescope drive motors.

2. Resolver System

Our angle encoder system is composed of a multi-speed resolver (figure 1) and a resolver-to-digital (RD) converter unit (figure 2). The resolvers are attached to a Yoke mount of the telescope and are connected by a rotor coupling to each axis. The relative position of the rotor and the stator is supported to the high degree of accuracy by a pair of bearing unit. The resolver bearing unit has a hollow shaft of 110 mm, through which optical fibers and cables can pass.

2.1 Multi-speed Resolver

The resolver is an inductive angle measuring device which has pairs of coils on each iron core of a rotor and stator. Our multi-speed resolver has two kinds of coils of two poles per turn (called 1X) and 256 poles (called 128X) are wound on each iron core of a rotor and stator. The purpose of two kinds of windings is to get an absolute angle of a turn with 1X and to improve angular resolution with 128X. Rotor rotation of a 1/128 turn (2.8125 deg) produces one cycle of amplitude variation of output signal in the 128X winding. When a winding on a rotor is excited with an AC reference signal (usually at frequency $f = 400$ Hz),

$$e_i = E \sin 2\pi ft \quad [\text{V}], \quad (1)$$

a sinusoidal voltage is also induced in stator windings. Two output voltages (e_s and e_c) in the two stator windings, which are placed perpendicular to each other, vary according to the sine and cosine of the shaft angle θ :

$$e_s = K_s e_i \sin(N\theta + \alpha_s) \quad [\text{V}], \quad (2)$$

$$e_c = K_c e_i \cos(N\theta + \alpha_c) \quad [\text{V}], \quad (3)$$

where K_s and K_c are a transformation ratio, N is a number of winding pair ($N = 1$ for 1X and $N = 128$ for 128X), and α_s and α_c are angle offsets. For an ideal resolver, the constants K_s and K_c are equal and the angles α_s and α_c are zero. Thus the output voltage ratio,

$$\frac{e_s}{e_c} = \tan N\theta, \quad (4)$$

is independent of the reference signal and depends only upon the shaft angle.

2.2 RD converter

Figure 2 shows a block diagram of the RD converter unit. The unit has three functions. First, angle signals of 1X and 128X resolver windings are converted into 7 bits and 18 bits signals, respectively. An absolute angle readout of 25 bits is obtained by combining two outputs of 1X and 128X. Second, the readout is corrected using a look-up table of angle errors at 2^{14} points per rotation (every about 80") stored in the PROM of the encoder electronics (hereafter, called the PROM correction). Finally, the data are transferred to the control equipment of the radio telescope. The angle data are held and read every 10 milli-second by the telescope control unit.

The RD converters used in our system are of tracking type. They are insensitive to environmental changes, such as temperature range, reference voltage tolerance, power supply fluctuations, etc. The frequency of operation can be changed in the range between 400 and 2000 Hz, in order to tune to minimize errors.

2.3 Resolver Error Characteristics

Output AC effective voltages which vary with a shaft angle are sinusoidal for an ideal resolver. In practice, they have distortions induced by several causes, for example, a misalignment between a ring of coils and a centerline of a hollow shaft (eccentricity error), or imperfection of coil shapes and slot shapes of rotor and stator. The rotor and stator have 256 and 296 slots, respectively. These misalignments and imperfections give small deviations of the transformation ratios among the individual coils. Since coils are connected in

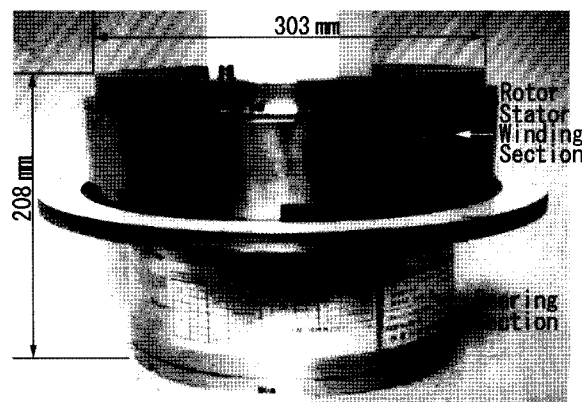


Fig. 1. A newly developed resolver with an accuracy of 30 mas rms.

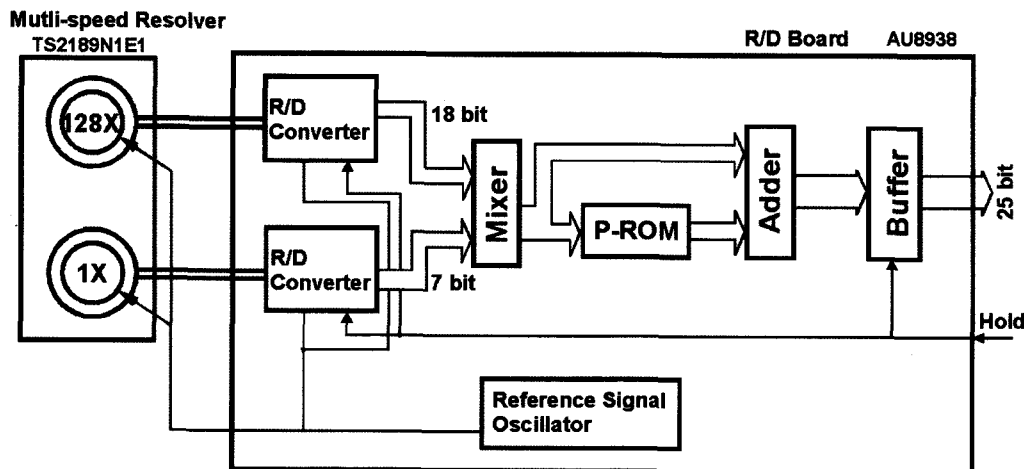


Fig. 2. A block diagram of a resolver-to-digital converter system.

series, these deviations are not localized, but are of periodic nature. The periodic error is the very distinctive feature of resolver. In order to achieve high accuracy and stability, it is important to identify error sources and to characterize them. The output voltage is usually written by following equations (e.g., Masaki 1999):

$$e_s = E_d + E_0(1 + \rho)\sin(\theta + \phi) + \sum_{j=1}^{\infty} E_{sj}\sin j\theta \quad [\text{V}] \quad (4)$$

$$e_c = E_0\cos\theta + \sum_{j=1}^{\infty} E_{cj}\cos j\theta \quad [\text{V}] \quad (5)$$

where E_d is a D.C. drift offset, $E_0 = K^*e_s$, ρ is an unbalance transformation ratio between sine and cosine output voltages, ϕ is non-orthogonality of the sine and cosine outputs, and E_{sj} and E_{cj} are errors due to mechanical misalignments and imperfections in sine and cosine outputs, respectively. Most of the terms are very small, but those for the misalignment between a ring of coils and a centerline of a hollow shaft ($j=1$ and 2) and those for the slot imperfection of iron core ($j=256$ and 296). Assuming that the ideal output angle θ has a small error of ϵ ,

$$\frac{e_s}{e_c} = \tan(\theta + \epsilon), \quad (6)$$

and $E_d/E_0 = \gamma$, ρ , and ϕ are also small, we obtain an error equation from equation (4) and (5).

$$\epsilon \approx \gamma\cos\theta + \frac{1}{2}[\rho\sin 2\theta + \phi(1 + \cos 2\theta)] + \sum_{j=1}^{\infty} \delta_j \sin(j\theta + \alpha_j) \quad (7)$$

where α_j and δ_j are phases and amplitudes of error components for errors due to mechanical misalignments and imperfections, respectively. In the development of our resolvers, the error budgets were given for these individual error sources using experiment data obtained with a similar resolver of a 1X-64X type.

2.4 Flexible Coupling

Besides the errors mentioned above, the reversal error is also a key which governs the antenna system performance. Measuring error that results from approaching a position from different directions is related to torsional stiffness of a coupling and the maximum static friction of the bearing unit. The former is $4.6 \text{ N m arcsec}^{-1}$, and the latter is 0.3 N m . Therefore, the maximum error is about 70 mas .

3. Measurements

3.1 Angle calibration system

All the measurements shown in this report were made with an angle calibration instrument that is well calibrated and maintained in a laboratory at Shizuoka Institute of Science and Technology (Masuda and Kajitani 1993). The measurement accuracy of the calibration system was presumed to be approximately 50 mas peak-to-peak. Using the time conversion method, relative angle position errors can be measured with a resolution of 1 mas . The rotation speed for the measurements was 0.1 rpm ($0.6 \text{ degree s}^{-1}$).

3.2 Resolver Error Pattern

The measured error pattern of the azimuth encoder is shown in the left panel of figure 3. The measurement was made at 2^{14} points per rotation (every about $80''$). The peak-to-peak error amplitude was about 4 arcsec . The right panel of figure 3 shows the Fourier component of the error. The figures clearly show that these errors are of periodic nature. The amplitudes of dominant components are listed in table 1. The amplitude of the first order error, which is due to machining accuracy and bearing rotational accuracy, are 1200 and

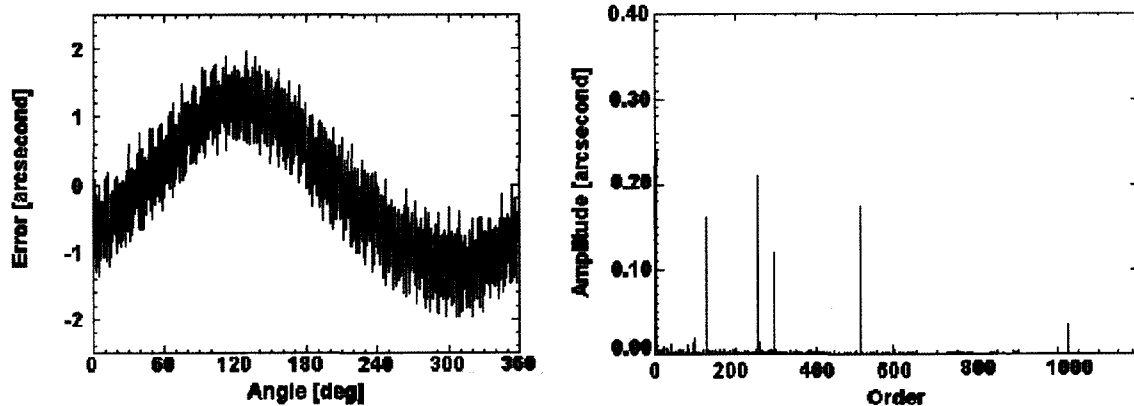


Fig. 3. Measurement of raw readout of the azimuth encoder (left) and its Fourier components (right).

Table 1. Measured amplitudes of periodic angle errors for the azimuth and elevation encoders.

Order	Amplitude of Error [milli-arcsecond]	
	Azimuth Encoder	Elevation Encoder
1 st	1,200	359
2 nd	80	94
3 rd	36	6
128 th	253	238
256 th	210	143
296 th	242	699
512 th	173	96

360 mas for the azimuth and elevation encoders, respectively. The error components of the 128th order, which is due to D.C. offset, are about 250 mas. The 256th order harmonic error, which is due to unbalance of the output voltages, non-orthogonality of the two outputs, and the rotor slot imperfection, are 210 and 143 mas. The amplitudes of the 296th order harmonic error by the slot imperfection of the stator were 242 mas and 699 mas for the azimuth and elevation encoders, respectively. In addition, the error has been composed of multiple components of these higher harmonic.

Similar resolvers made for the 45-m telescope in 1988 had an error amplitude of 13" in raw readout. The accuracies of the new resolvers are clearly improved. They are about 3 times as high as that of the former. The improvement seems to be due to new winding arrangements, namely sinusoidally distributed winding on fractional slot (Masaki 1999). The other causes of the improvement would be cutting precision of stator/rotator core and rotational accuracy of the bearing unit.

3.3 Accuracy after PROM correction

Five measurements of the error pattern were repeated while the relative orientation angle between the resolver shaft and the angle calibration instrument is shifted by

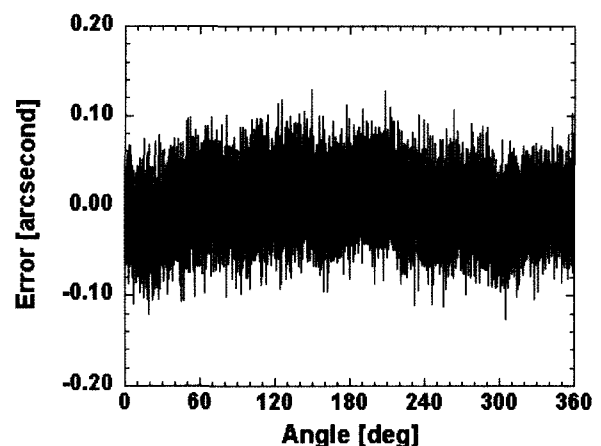


Fig. 4. Angle errors of readouts after PROM compensation.

72 degree. The periodic errors except for $72/n$ degree components with the calibration instrument, if any, are suppressed by average of these five measurements. The averaged error pattern is stored in the PROM. Figure 4 shows a subsequent measurement of the angle error after the PROM correction. The error was measured to be 30 mas rms and 260 mas peak-to-peak.

The achieved accuracy of 30 mas rms is 1/5 of the specified value in the LMSA/ALMA project. The 4" peak-to-peak error of the resolver was reduced to less than 1/15 by the PROM correction. The accuracy of the resolver system was repeatedly measured for several days. We confirmed the reproducibility level to be equal to the accuracy level. This suggests that the resolver bearing unit rotates accurately without irregular motion. Runout components which are not synchronous with rotation are very small.

3.4 Error due to shaft misalignment

When an angle encoder is installed on a telescope mount, shaft misalignment is inevitable. To accommo-

date the misalignment, collinear axes are connected with a flexible coupling. Our 10-m antenna has alignment adjusters for the azimuth axis, but no adjusters for the elevation axis. We need to measure changes of error characteristics due to shaft misalignment.

There are two sources of error associated with shaft misalignment. They are transmission error of the flexible coupling and error due to displacement of a resolver bearing unit.

Figure 5 shows Fourier components of error amplitudes induced by a radial misalignment of 0.10mm. Only the changes of 78 mas and 28 mas were observed in the first and second order components, respectively. No changes larger than 3 mas were observed in the high order components. In practice, the first order component of the above errors is usually removed in a telescope control computer programme together with pointing errors due to antenna axis misalignment, radio beam tilt due to gravitational deformation, etc. These results suggest that the integration simply by the fitting could ensure the accuracy necessary. It would be a great help for us that no finer alignment for centering is required.

Figure 6 shows amount of change of the first order harmonic component vs. radial misalignment. The amplitude of angle error increases with the displacement. The error amplitude is given as

$$\epsilon \approx \frac{\pi \delta}{4NR_s}, \quad (8)$$

where δ is the radial shift of the rotor shaft centerline, N is a number of winding pair ($N = 128$), and R_s is a radius of stator (125 mm) (Masaki 1999). From the observed error amplitude, we find that the radial shift of the rotor centerline δ is about $8 \mu\text{m}$, small compared with the radial misalignment of $100 \mu\text{m}$.

3.5 Temperature dependence of error pattern

The telescope is operated in the open air. The expected temperature variation ranges from -20 to $+20$ degree Celsius. Since there is no temperature control for the resolvers, it is our great concern how large the periodic error pattern of the resolvers changes with temperature.

We measured the error patterns before and after the temperature of the laboratory room changed by 8 degree. Comparisons of each Fourier component of the error patterns have revealed variations of 13 – 32 mas in the 1st, 2nd, and 3rd components and a small change of 6 mas in the 256th components. Since there are many potential causes for the changes of the low Fourier component in both the resolver itself and the angle calibration system, it is difficult to estimate variations of the

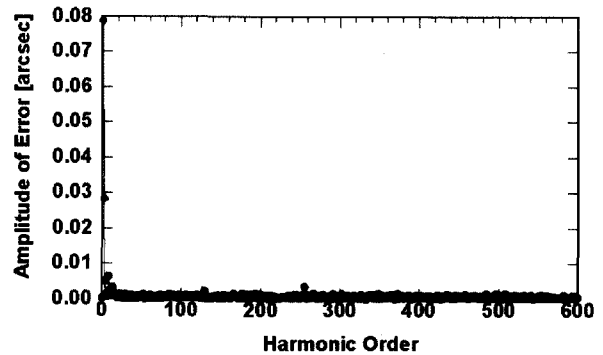


Fig. 5. Fourier components of error due to shaft radial misalignment of 0.10 mm.

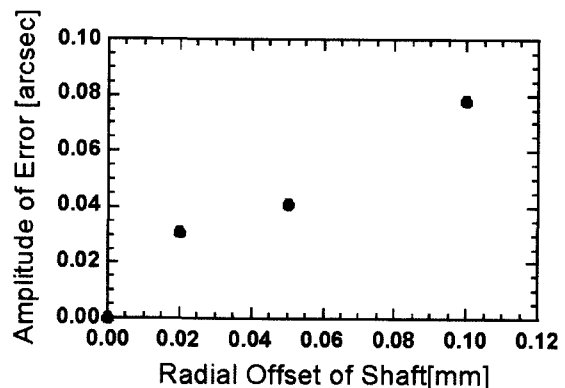


Fig. 6. Increase of error due to shaft radial misalignment.

error intrinsic to the resolver. The variation of the 256th component may be due to changes of winding shapes by different thermal coefficients among windings, stator/rotor cores, and varnish material.

It is important to note that the calibrations were made at a room temperature of about $+20$ degree Celsius. At the lower end of -20 degrees Celsius, the 256th component would increase to amplitude of 30 mas, but it would be a negligible contribution.

4. Concluding Remarks

We have measured angle error characteristics of newly developed resolvers for NRO 10-m submillimeter telescope. We have found they have an accuracy of 30 mas rms and 260 mas peak-to-peak, which is well below the specified value in the LMSA/ALMA project. The 4" peak-to-peak error in the raw readout is reduced to less than 1/15 by the PROM correction. We have also found that shaft misalignment causes only small changes of error pattern, which enables us to install the resolver simply by the fitting. The temperature dependence of error pattern also seems to be small enough for the operation temperature range specified in the project. The current achievement is a result of advanced design

technique of a resolver and R/D converter, a high precision bearing unit, and a shaft coupler in a decade.

The authors wish to thank Mr. K. Toyotake for his assistance during the measurements at Shizuoka Institute of Science and Technology.

References

- Cheng, J., and Kingsley, J. 1998, "12-m Antenna Design for a Joint US-European Array," in *Advance Technology MMW, Radio, and Terahertz Telescopes*, ed. T.G. Philips, Proc. SPIE **3357**, 671–685.
- Ishiguro, M., and the LMSA working group, 1998, "Japanese Large Millimeter and Submillimeter Array," in *Advance Technology MMW, Radio, and Terahertz Telescopes*, ed. T.G. Philips, Proc. SPIE **3357**, 244–253.
- Masaki, K. 1999, "Study on Development of High Accuracy Resolvers based on Spatial Harmonic Elimination," Ph. D. thesis, Shinshu Univ. (in Japanese).
- Matsuda, T., and Kajitani, M. 1993, "High Accuracy Calibration System for Angular Encoders," *J. Robotics and Mechatronics* **5**, 448–452.
- Ukita, N. 1999, "Thermal Effects on the Pointing of the Nobeyama 45-m Telescope," in *Publ. Natl. Astron. Obs. Japan* **5**, 139–147.
- Ukita, N. et al. 2000, "NRO 10-m submillimeter telescope," in *Radio Telescopes*, ed. H.R. Butcher, Proc. SPIE **4015**, 177–184.
- Ukita, N., and Tsuboi, M. 1994, "A 45-m Telescope with a Surface Accuracy of $65\mu\text{m}$," in *Proc. of the IEEE* **82**, 725–733.